Einstein-Podolsky-Rosen Spatial Entanglement in Ordered and Anderson Photonic Lattices

G. Di Giuseppe,[1,2] L. Martin,[1] A. Perez-Leija,[1,3] R. Keil,[3] F. Dreisow,[3] S. Nolte,[3]
A. Szameit,[3] A. F. Abouraddy,[1] D. N. Christodoulides,[1] and B. E. A. Saleh[1]

[1]*CREOL, The College of Optics & Photonics, University of Central Florida, Orlando, Florida 32816, USA*
[2]*School of Science and Technology, University of Camerino, 62032 Camerino, Macerata, Italy*
[3]*Institute of Applied Physics, Friedrich-Schiller-Universität Jena, Max-Wien-Platz 1, 07743 Jena, Germany*
(Received 19 November 2012; revised manuscript received 11 February 2013; published 10 April 2013)

We demonstrate quantum walks of a photon pair in a spatially extended Einstein-Podolsky-Rosen state coupled into an on-chip multiport photonic lattice. By varying the degree of entanglement we observe Anderson localization for pairs in a separable state and Anderson colocalization for pairs in an Einstein-Podolsky-Rosen entangled state. In the former case, each photon localizes independently, while in the latter neither photon localizes, but the pair colocalizes—revealing unexpected survival of the spatial correlations through strong disorder.

DOI: 10.1103/PhysRevLett.110.150503 PACS numbers: 03.67.Bg, 42.25.Dd, 42.65.Lm, 72.15.Rn

Quantum information processing promises exponential speedup of intractable computational problems, secure cryptographic key distribution, and exotic communications protocols such as teleportation [1]. Manipulating entangled multipartite quantum states on a chip is now paving the way towards scalable platforms for quantum information processing and quantum communications [2–5]. Among the potential physical platforms, photonic realizations offer benefits in terms of simplicity of generating and transforming entangled quantum states [6]. Advances in micro- and nanofabrication have recently enabled a new generation of on-chip quantum photonic devices that may enable large-scale linear quantum computation [7] and the observation of fundamental processes such as quantum walks [8,9].

To fully exploit the information-carrying capacity of any physical system, all relevant degrees of freedom, whether spin, frequency, or spatial, must be utilized. Thus far, photon polarization [10] or two-path realizations [5] have been the preferred on-chip qubit embodiment. The quest for increasing the information-carrying capacity of a single photon necessitates the use of other degrees of freedom that offer higher dimensionality. It is thus important to explore new classes of integrated photonic configurations capable of harnessing such high-dimensional degrees of freedom. Clearly, the benefits accrued will be even greater if entanglement is utilized in such large-dimensional systems. In particular, spatially entangled photon pairs [11]—whose counterintuitive properties were the starting point of the Einstein-Podolsky-Rosen (EPR) gedankenexperiment [12]—naturally inhabit a high-dimensional Hilbert space [13,14]. To date, realizations of integrated photonic quantum circuits first project the spatial degree of freedom onto a single mode, thereby stripping the spatial entanglement, in order to couple into on-chip waveguide systems [5,10,15].

Quite recently, the study of the evolution of two-photon states in one-dimensional waveguide lattices was suggested by Bromberg *et al.* [16]. Here we experimentally demonstrate large-scale quantum walks using two-photon spatially extended EPR states launched into on-chip multiport lattice circuits with and without disorder. In one configuration, quantum walks through a periodic waveguide array convert spatially correlated EPR pairs into anticorrelated pairs—a spatially extended inverse of Hong-Ou-Mandel interference [17]. In a different configuration, a lattice with controllable disorder halts the spreading of each photon of a pair in a separable state—leading to the first demonstration of Anderson localization (AL) [18] at the single-photon level. When entangled EPR photons are launched into this array, we observe a new disorder-mediated two-photon interference effect. The extended EPR photons do not localize. In this case, their spatial correlations unexpectedly survive the disordered quantum random walk, resulting in localization in fourth-order correlation space, or *colocalization* [19,20].

In our experiment (Fig. 1-i) we produce EPR photon pairs by optical spontaneous parametric down-conversion from a nonlinear crystal (NLC) [11]. These entangled photon pairs are then imaged to the input plane of an integrated multiport photonic lattice. Entangled quantum walk experiments were carried out in three different lattices, each consisting of a large array of 101 evanescently coupled, parallel, identical, single-mode, low-loss optical waveguides inscribed in silica glass [21]. In this setting, the waveguides have identical propagation constants, and the inter-waveguide coupling is determined by their separation (Fig. 1-ii and Fig. 1-iii).

The evolution along z of the quantized-field operators $a_n^\dagger$ in the nth waveguide in this tight-binding lattice is determined by the Heisenberg equation of motion in the interaction picture [16], $-i\frac{da_n^\dagger}{dz} = \kappa_{n,n-1}a_{n-1}^\dagger + \kappa_{n+1,n}a_{n+1}^\dagger$, where $\kappa_{n,n-1}$ is the coupling coefficient between adjacent sites. Integration of this equation yields $\mathbf{A}^\dagger(z) = \hat{\mathbf{U}}(z)\hat{\mathbf{A}}^\dagger(0)$, where $\hat{\mathbf{A}}^\dagger(z) = [a_n^\dagger(z)]_{n=1}^N$, $\hat{\mathbf{U}}(z) = e^{i\hat{\mathbf{H}}z}$, and

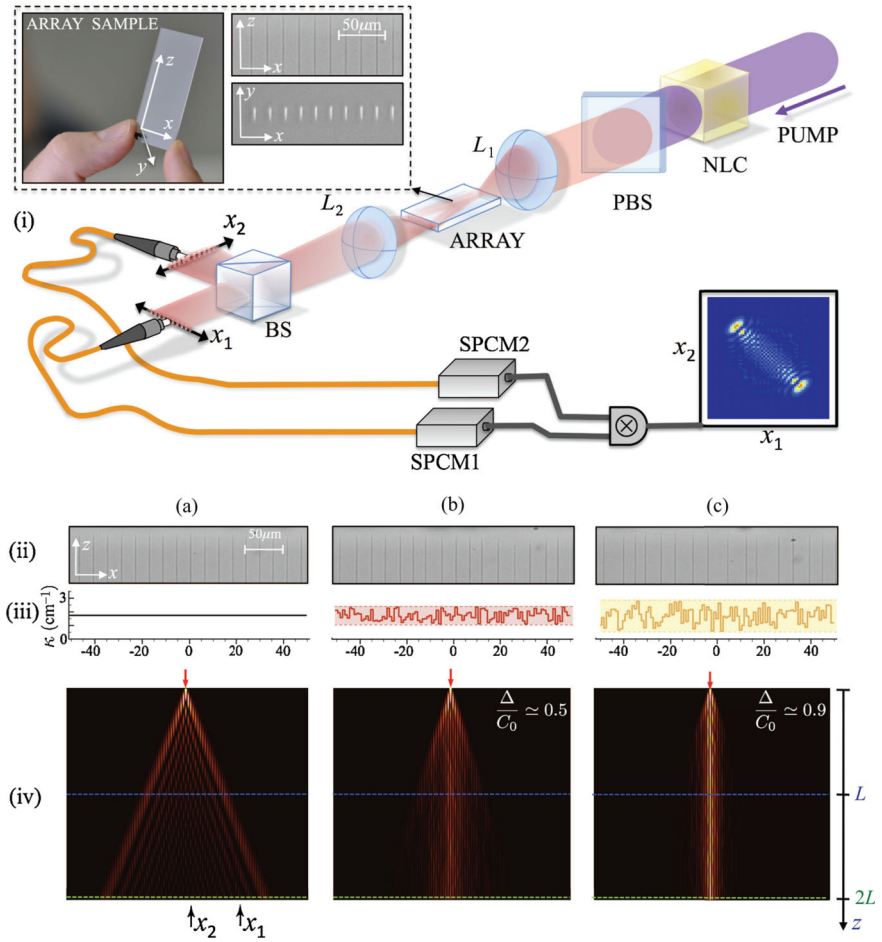

FIG. 1 (color online). (i) Experimental setup. A pump laser incident on a NLC generates spatially entangled photon pairs that are coupled into a waveguide array using a lens L_1 (an achromatic doublet, focal length 30 mm) in an imaging configuration. The distance from the nonlinear crystal to L_1 and the distance from L_1 to the waveguide array were chosen to demagnify the spatial extent of the photon pairs by a factor of 4. A lens L_2 (an achromatic doublet, focal length 40 mm) images the photon pairs emerging from the array with a magnification factor of 6.5 to two identical planes x_1 and x_2 separated using a beam splitter (BS), and are collected by two scanning fibers coupled to detectors SPCM1 and SPCM2. A coincidence circuit provides the correlation function $G^{(2)}(x_1, x_2)$. The pump beam is removed after the NLC using a polarizing beam splitter (PBS). Inset: Photograph of the waveguide array sample (left), a phase-contrast microscope image of a section of the periodic array taken from the top of the array showing the waveguides along z (top right), and an optical micrograph of white light emerging from the periodic array output (bottom right). (ii) Phase-contrast microscope images of a section of each waveguide array. (iii) Values of the nearest-neighbor coupling coefficients for each array. (iv) Calculated evolution of a one-photon state along each waveguide array when a single waveguide is excited. Distances $L = 5$ cm (the physical length of the arrays) and $2L$ are highlighted. Columns: (a) periodic, (b) weakly disordered, and (c) highly disordered arrays.

$\hat{\mathbf{H}}$ represents the coupling-coefficient matrix. In experiments using two-photon states, this transformation applies to the quantized field operators of each photon.

In our work we consider three such arrays of length $L = 5$ cm: a periodic array $\kappa_{n,n-1} = \kappa_o$, $\forall\, n$ (Fig. 1-ii-a); a weakly disordered array with coupling constants chosen from a uniform random distribution $\kappa \in [\kappa_o - \Delta, \kappa_o + \Delta]$ with mean κ_0 and normalized width $\Delta/\kappa_o = 0.5$ (Fig. 1-ii-b); and a strongly disordered array with $\Delta/\kappa_o = 0.9$ (Fig. 1-ii-c). The array output plane is imaged to two identical planes, x_1 and x_2 (Fig. 1-i). Two fibers connected to single-photon-sensitive detectors are scanned in these planes to collect the emerging photons at the imaged waveguide locations in order to register the coincidence rate $G^{(2)}(x_1, x_2)$ [22]. The dynamics of one-photon states when launched into a single waveguide are depicted in Fig. 1-iv for these three cases.

The entangled photon pairs produced in our experiment are in a quantum-correlated two-photon state as previously demonstrated [11,23]. Each pair is always injected together into a waveguide. This waveguide can be any of the $N = 101$ sites covered by the spatial extent M of the state. The two-photon EPR state, or multipath entangled state, covering M discrete lattice points takes the form

$$|\Psi_{\mathrm{EPR}}\rangle = \frac{1}{\sqrt{M}}\{|2_1, 0_2, \cdots, 0_M\rangle + |0_1, 2_2, \cdots, 0_M\rangle + \cdots + |0_1, 0_2, \cdots, 2_M\rangle\}, \quad (1)$$

where the indices refer to the sites. The quantum correlations in this spatially extended state $|\Psi_{\mathrm{EPR}}\rangle$ are such that the two photons are always on the same lattice site, but with equal probability $\frac{1}{M}$ of being at any of the M excited sites. In our experiments, $M = 20$ and the uniform probability distribution is approximated by a truncated broad Gaussian distribution. In contrast, a separable two-photon state is excited if they are both launched into a single waveguide k

$$|\Psi_{\mathrm{sep}}\rangle = |0_1, 0_2, \cdots, 0_{k-1}, 2_k, 0_{k+1}, \cdots, 0_M\rangle. \quad (2)$$

In this separable state, the two photons are independent. We stress that current experimental approaches that make use of integrated devices have so far relied on first coupling the photon pairs into a single-mode fiber, which destroys their spatial correlations. Here we obviate this limitation through free-space imaging of the EPR state from the NLC to the chip, thereby loading spatial entanglement into the photonic circuit. This scheme allows the high dimensionality of the EPR state in Eq. (1) to be exploited in an integrated quantum photonic arrangement to observe entangled quantum walks.

The propagation dynamics of a two-photon state along the three arrays depends on the initial state. If $|\Psi_{\mathrm{sep}}\rangle$ is injected into a single waveguide in any of the arrays, the output coincidence rate separates into a product $G^{(2)}(x_1, x_2) = G^{(1)}(x_1, x_1)G^{(1)}(x_2, x_2)$ of single-photon distributions $G^{(1)}(x_1, x_1)$ and $G^{(1)}(x_2, x_2)$ [11,24]. When light in the state $|\Psi_{\mathrm{EPR}}\rangle$ is coupled into the array, $G^{(2)}(x_1, x_2)$ no longer factorizes and the dynamics are altogether different.

Experiment.—The experimental setup is illustrated in Fig. 1. Photon pairs are produced via collinear degenerate type-I optical spontaneous parametric down conversion from a $LiIO_3$, 1.5-mm thick nonlinear crystal excited with a pump laser (CW Coherent Cube laser diode, 80-mW power, 404-nm wavelength, vertically polarized). The photon pairs (horizontally polarized, centered at 808 nm) are coupled into the waveguide array using an achromatic doublet lens of 30-mm focal length in a telescopic imaging arrangement. The pump beam is removed after the NLC using a Glan-Thompson polarizing beam splitter and a red long-pass filter after the array. This arrangement is similar to that previously used in Ref. [23] where we demonstrated a violation of Bell's inequality, thereby ensuring the high degree of entanglement of the state produced here. The photon pairs emerging from the array are imaged using an achromatic doublet lens of 40-mm focal length to two identical planes x_1 and x_2 separated using a nonpolarizing BS and are collected by two fibers (multimode, 62.5-μm core diameter) coupled to single-photon-sensitive detectors SPCM1 and SPCM2 (Perkin-Elmer, SPCM-AQR-15-FC). A coincidence circuit measures the correlation function $G^{(2)}(x_1, x_2)$ using a 3-ns window. The waveguide elements, which are inscribed in silica glass, are all identical and single mode (width 4 μm, height 11 μm, NA 0.045, length 5 cm). In the periodic array, the center-to-center waveguide separation is 17 μm and the measured coupling coefficient $\kappa_o \approx 1.7\ \mathrm{cm}^{-1}$. The disordered arrays are implemented by varying the distance between adjacent guides such that a uniform distribution of the coupling κ is obtained [19,25]. In analyzing the data from these finite arrays, we have carried out simulations using the actual distribution of coupling coefficients. A more complete statistical analysis was carried out in Refs. [20,25].

Periodic array.—We first investigate the evolution of $|\Psi_{\mathrm{sep}}\rangle$ and $|\Psi_{\mathrm{EPR}}\rangle$ along the periodic array (Fig. 2): (i) When the $|\Psi_{\mathrm{sep}}\rangle$ state is excited, the measured coincidence rate $G^{(2)}(x_1, x_2)$ features four symmetric peaks (Fig. 2-iii-a) and is separable into the product of two pairs of ballistic peaks for each photon (Fig. 1-iv-a). These peaks

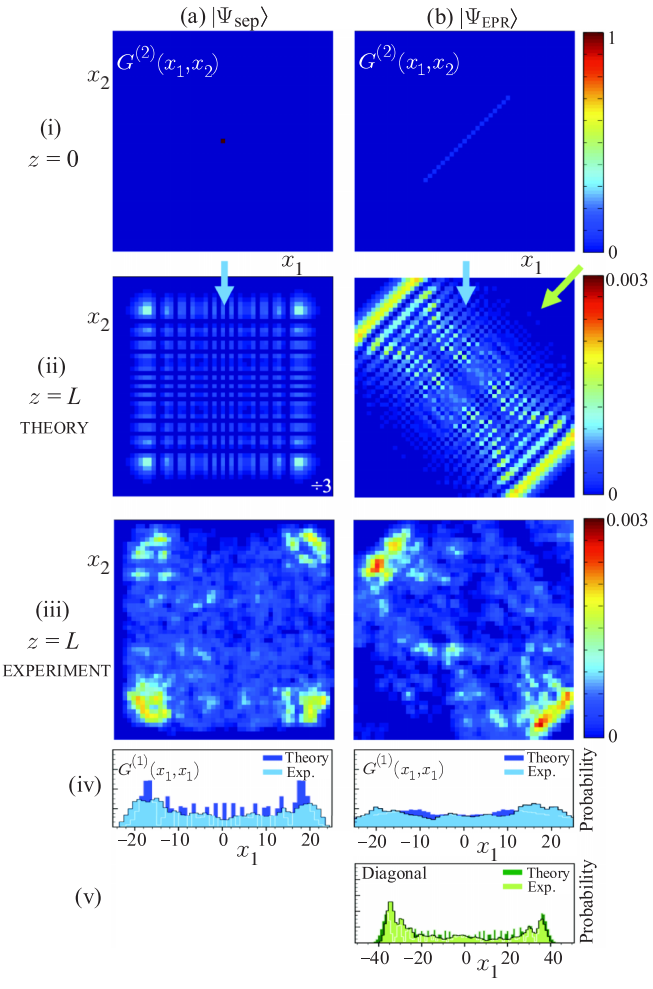

FIG. 2 (color online). Observation of the correlation function $G^{(2)}(x_1, x_2)$ in a periodic lattice. Column (a) corresponds to the separable state $|\Psi_{\mathrm{sep}}\rangle$ and column (b) to the entangled state $|\Psi_{\mathrm{EPR}}\rangle$. (i) Expected $G^{(2)}(x_1, x_2)$ at the input. (ii) Theoretical and (iii) measured coincidence rate at the output. (iv) Calculated and measured singles distribution $G^{(1)}(x_1, x_1)$ at the output. (v) Calculated and measured diagonals distribution at the output for $|\Psi_{\mathrm{EPR}}\rangle$. The width of the horizontal axis for x_1 in (v) is twice that in the rest of the figure.

signify that if a photon is detected on one side of the array, then its twin is equally likely to be detected on the same side (the diagonal peaks) or at its mirror symmetric location with respect to the input site (the off-diagonal peaks). As in the case of a beam splitter with a two-photon state at one input port, the two photons are equally likely to emerge from the same or different ports. Here the array plays the role of a spatially extended beam-splitting photonic circuit. Consequently, the singles distributions are identical to the single-photon (or classical) outcome $G^{(1)}(x_1, x_1)$ for the same array (Fig. 2-iv-a). This arrangement corresponds to a two-photon continuous quantum random walk [26,27], where each photon in the pair evolves independently. (ii) The two-photon dynamics are dramatically altered when $|\Psi_{\mathrm{EPR}}\rangle$ is excited instead. The two diagonal peaks that appear in the separable case are here suppressed (Fig. 2-ii-b and Fig. 2-iii-b), leaving only two prominent off-diagonal peaks, as predicted theoretically in Ref. [20]. Surprisingly, even though the two photons at the input are always in the same lattice site, at the end of the quantum walk they emerge from opposite sides of the array with respect to the center. Furthermore, $G^{(2)}(x_1, x_2)$ is not factorizable and the singles correspond to the evolution of a spatially extended mixed one-photon state (Fig. 2-iv-b). Nevertheless, examining the diagonal marginal distribution (diagonals), resulting from integrating $G^{(2)}$ along $x_1 = x_2$ [19], brings forth an unexpected result (Fig. 2-v-b). In general, the diagonals reveal the distribution of separations between the two photons emerging from the array. Here the diagonals distribution equals that resulting from the evolution of a one-photon state that is coupled into a single lattice site and after propagating for a distance $2L$—twice the length of the physical array [20]. The two off-diagonal peaks, along the $x_1 = -x_2$ axis, in the periodic array signify that the two photons always emerge on opposite sides of the array, although the pairs are coupled into the same waveguides at the input. In essence, this observation corresponds to the reverse of the usual two-photon Hong-Ou-Mandel interference effect [17] where two photons enter different ports of a beam splitter and emerge together from one of the output ports. Our arrangement realizes the inverse of this effect in a spatially extended configuration across the waveguide array.

Disordered array.—We now investigate how the two-photon quantum walk is affected in the extreme limit of a strongly disordered lattice that is expected to halt the spreading of single-photon states. In this regime, transverse photonic AL has been observed using classical states of light [24,25,28–30]. Using such a random array, we study quantum walks using both $|\Psi_{\mathrm{sep}}\rangle$ and $|\Psi_{\mathrm{EPR}}\rangle$. (i) In the separable case [Fig. 3(a)] we observe for the first time AL at the single-photon level. Both photons in this separable state undergo independently the localization process (Fig. 3-ii-a and Fig. 3-iii-a). (ii) In the spatially entangled case, neither of the spatially extended EPR photons localizes (as observed in the singles shown in Fig. 3-iii-b). In

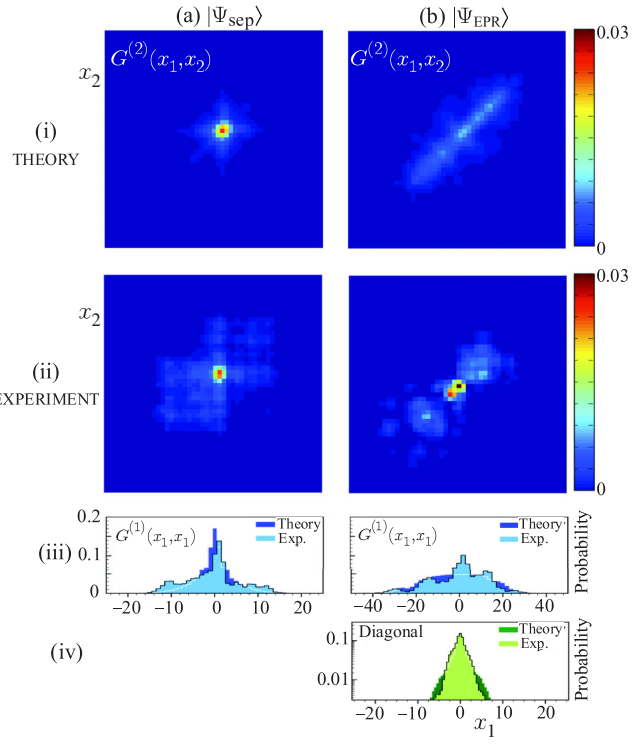

FIG. 3 (color online). Same as in Fig. 2 for the disordered Anderson lattice ($\Delta/\kappa_o = 0.9$).

fact $G^{(2)}(x_1, x_2)$ in this regime resembles that of the input EPR state (Fig. 2-i-b). In other words, the spatial correlations inherent in $|\Psi_{\mathrm{EPR}}\rangle$ survive even in the presence of such extreme disorder. This two-photon disorder-mediated interference effect leads to localization in correlation space as seen clearly in the diagonal distribution (Fig. 3-iv-b). The exponential localization in the latter figure is evident from the linear slope (triangular shape) in the logarithmic scale we used in plotting. Whether this newly observed absence of diffusion in correlation space is a form of AL remains an open question. The ''hot-spot''observed in the data in Fig. 3-ii-b is due to the deviation between the assumed flat distribution of the random coupling coefficients in theory and the actual values in the fabricated sample.

Weakly disordered array.—We have also performed similar measurements in an array with coupling coefficients (Fig. 1-iii-b) chosen such that a one-photon state coupled into a single waveguide will exhibit an output distribution $G^{(1)}(x_1, x_1)$ that combines both ballistic propagation and AL features after propagating the physical distance L, but demonstrates a strong AL signature after twice the distance $2L$. The measurements of $G^{(2)}(x_1, x_2)$ for this array are shown in Fig. 4. For excitation in the state $|\Psi_{\mathrm{sep}}\rangle$, $G^{(2)}(x_1, x_2)$ does not localize as occurs in the case of the strongly disordered array [Fig. 3(a)]. The singles $G^{(1)}(x_1, x_1)$ in Fig. 4-iii-a reveal ballistic and AL features as is expected from the calculation of the evolution shown in Fig. 1-iv-b. When the photon pairs are coupled into 20

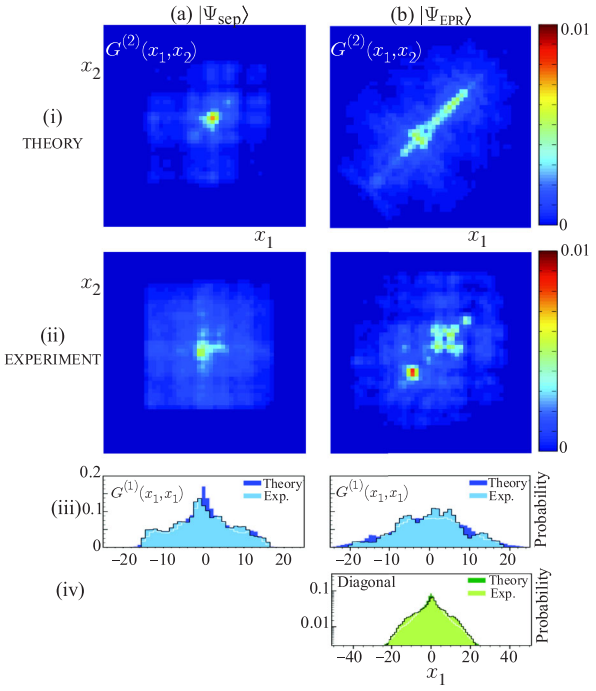

FIG. 4 (color online). Same as in Fig. 2 for the weakly disordered Anderson lattice ($\Delta/\kappa_o = 0.5$).

adjacent waveguides, and hence $|\Psi_{\mathrm{EPR}}\rangle$ is excited, the measured $G^{(2)}(x_1, x_2)$ is shown in Fig. 4-ii-b. The singles $G^{(1)}(x_1, x_1)$, Fig. 4-iii-b, reveal an extended distribution of both photons with no sign of localization. On the other hand, when the diagonals are examined (Fig. 4-iv-b, shown in logarithmic scale), we observe the localized state distribution that results from exciting a single waveguide in this array after propagating a distance $2L$, and hence exhibits a clear AL signature.

Conclusion.—We have demonstrated deterministic and disordered quantum walks on large-scale on-chip lattices implemented on a spatially extended two-photon EPR state. Other entangled states besides $|\Psi_{\mathrm{EPR}}\rangle$ may also be launched into such multiport structures by manipulating the relative complex weights of the two-photon basis functions either at the NLC or using the imaging system. In the process, we observed AL at the single-photon level and also a new form of localization in correlation space resulting from the quantum random walk of an EPR photon pair on a disordered lattice. In principle, these systems may be adapted to incorporate other optical degrees of freedom, such as polarization and frequency, further expanding the dimensionality of the Hilbert space. Moreover, two-dimensional realizations of such networks, permanent or reconfigurable [31], can also be utilized for implementing more sophisticated operations and quantum random walks.

[1] M. A. Nielsen and I. L. Chuang, *Quantum Computation and Quantum Information* (Cambridge University Press, Cambridge, England, 2000).
[2] R. Folman, P. Kruger, J. Schmiedmayer, J. Denschlag, and C. Henkel, Adv. At. Mol. Opt. Phys. **48**, 263 (2002).
[3] J. T. Merrill *et al.*, New J. Phys. **13**, 103005 (2011).
[4] J. Majer *et al.*, Nature (London) **449**, 443 (2007).
[5] A. Politi, M. J. Cryan, J. G. Rarity, S. Y. Yu, and J. L. O'Brien, Science **320**, 646 (2008).
[6] D. Bouwmeester, A. K. Ekert, and A. Zeilinger, *The Physics of Quantum Information* (Springer, Berlin, 2000).
[7] E. Knill, R. Laflamme, and G. J. Milburn, Nature (London) **409**, 46 (2001).
[8] Y. Aharonov, L. Davidovich, and N. Zagury, Phys. Rev. A **48**, 1687 (1993).
[9] H. B. Perets, Y. Lahini, F. Pozzi, M. Sorel, R. Morandotti, and Y. Silberberg, Phys. Rev. Lett. **100**, 170506 (2008).
[10] L. Sansoni, F. Sciarrino, G. Vallone, P. Mataloni, A. Crespi, R. Ramponi, and R. Osellame, Phys. Rev. Lett. **105**, 200503 (2010).
[11] A. F. Abouraddy, M. B. Nasr, B. E. A. Saleh, A. V. Sergienko, and M. C. Teich, Phys. Rev. A **63**, 063803 (2001).
[12] A. Einstein, B. Podolsky, and N. Rosen, Phys. Rev. **47**, 777 (1935).
[13] C. K. Law and J. H. Eberly, Phys. Rev. Lett. **92**, 127903 (2004).
[14] A. C. Dada, J. Leach, G. S. Buller, M. J. Padgett, and E. Andersson, Nat. Phys. **7**, 677 (2011).
[15] J. L. O'Brien, A. Furusawa, and J. Vukovic, Nat. Photonics **3**, 687 (2009).
[16] Y. Bromberg, Y. Lahini, R. Morandotti, and Y. Silberberg, Phys. Rev. Lett. **102**, 253904 (2009).
[17] C. K. Hong, Z. Y. Ou, and L. Mandel, Phys. Rev. Lett. **59**, 2044 (1987).
[18] P. W. Anderson, Phys. Rev. **109**, 1492 (1958).
[19] Y. Lahini, Y. Bromberg, D. N. Christodoulides, and Y. Silberberg, Phys. Rev. Lett. **105**, 163905 (2010).
[20] A. F. Abouraddy, G. Di Giuseppe, D. N. Christodoulides, and B. E. A. Saleh, Phys. Rev. A **86**, 040302(R) (2012).
[21] A. Szameit, F. Dreisow, R. Pertsch, S. Nolte, and A. Tünnermann, Opt. Express **15**, 1579 (2007).
[22] R. J. Glauber, Phys. Rev. **130**, 2529 (1963).
[23] T. Yarnall, A. F. Abouraddy, B. E. A. Saleh, and M. C. Teich, Phys. Rev. Lett. **99**, 170408 (2007).
[24] T. Schwartz, G. Bartal, S. Fishman, and M. Segev, Nature (London) **446**, 52 (2007).
[25] L. Martin *et al.*, Opt. Express **19**, 13 636 (2011).
[26] A. Peruzzo *et al.*, Science **329**, 1500 (2010).
[27] A. Schreiber, A. Gábris, P. P. Rohde, K. Laiho, M. Štefaňák, V. Potoček, I. J. C. Hamilton, and C. Silberhorn, Science **336**, 55 (2012).
[28] H. De Raedt, A. Lagendijk, and P. de Vries, Phys. Rev. Lett. **62**, 47 (1989).
[29] Y. Lahini, A. Avidan, F. Pozzi, M. Sorel, R. Morandotti, D. N. Christodoulides, and Y. Silberberg, Phys. Rev. Lett. **100**, 013906 (2008).
[30] A. Szameit, Y. V. Kartashov, P. Zeil, F. Dreisow, M. Heinrich, R. Keil, S. Nolte, A. Tünnermann, V. A. Vysloukh, and L. Torner, Opt. Lett. **35**, 1172 (2010).
[31] P. J. Shadbolt, M. R. Verde, A. Peruzzo, A. Politi, A. Laing, M. Lobino, J. C. F. Matthews, M. G. Thompson, and J. L. O'Brien, Nat. Photonics **6**, 45 (2012).